ELSEVIER

Earth and Planetary Science Letters 185 (2001) 369–382

EPSL

www.elsevier.com/locate/epsl

Holocene rainfall variability in southern Chile: a marine record of latitudinal shifts of the Southern Westerlies

Frank Lamy *, Dierk Hebbeln, Ursula Röhl, Gerold Wefer

Fachbereich Geowissenschaften, Universität Bremen, Postfach 33 04 40, 28334 Bremen, Germany

Received 10 May 2000; received in revised form 5 December 2000; accepted 9 December 2000

Abstract

Geochemical and clay mineral parameters of a high accumulation marine sediment core from the Chilean continental slope (41°S) provide a 7700 yr record of rainfall variability in southern Chile related to the position of the Southern Westerlies. We especially use the iron content, measured with a time-resolution of ca. 10 yr on average, of ^{14}C-accelerator mass spectrometry dated marine sediments as a proxy for the relative input of iron-poor Coastal Range and iron-rich Andean source rocks. Variations in this input are most likely induced by rainfall changes in the continental hinterland of the core position. Based on these interpretations, we find a pronounced rainfall variability on multi-centennial to millennial time-scales, superimposed on generally more arid conditions during the middle Holocene (7700 to 4000 cal yr B.P.) compared to the late Holocene (4000 to present). This variability and thus changes in the position of the Southern Westerlies are first compared to regional terrestrial paleoclimate data-sets from central and southern Chile. In order to derive possible wider implications and forcing mechanisms of the Holocene latitudinal shifts of the Southern Westerlies, we then compare our data to ice-core records from both tropical South America and coastal Antarctica. These records show similar bands of variability centered at ca. 900 and 1500 yr. Comparisons of band pass filters suggest a close connection of shifts of the Southern Westerlies to changes within the tropical climate system. The correlation to climate conditions in coastal Antarctica shows a more complicated picture with a phase shift at the beginning of the late Holocene coinciding with the onset of the modern state of El Niño-Southern Oscillation system. The presented data provide further evidence that the well known millennial-scale climate variability during the last glacial continued throughout the Holocene.

Keywords: paleoclimatology; Holocene; circulation; Chile

1. Introduction

Unlike the last glacial, with its large millennial-scale, abrupt climatic shifts (e.g. [1]), the Holocene climate is classically seen to be anomalously stable (e.g. [2]). Recently, increasing evidence for a less stable Holocene climate comes from studies on ice-cores of both Greenland [3,4] and Antarctica [5], as well as from marine sediment cores of the North Atlantic region (e.g. [6]) and the Arabian Sea (e.g. [7]). These studies suggest climate cycles on time-scales ranging from millennial to multi-centennial, which might be a continuation of the well-known rapid climate changes of the last glacial and deglaciation which have been

* Corresponding author. Tel.: +49-421-2187759; Fax: +49-421-2183116; E-mail: frankl@allgeo.uni-bremen.de

0012-821X/01/$ – see front matter
PII: S0012-821X(00)00381-2

found in paleoclimate records from nearly all around the world [8]. Recent modeling studies also suggest significant changes of the El Niño-Southern Oscillation system (ENSO) [9] on millennial time-scales during the Holocene.

The principal obstacle in investigating Holocene climate change is the lack of well-dated high resolution geologic sequences from climate sensitive regions with responsive geologic recording systems. One such region is in the mid-latitudes of Chile where an extreme north–south precipitation gradient is controlled by the latitudinal position of the Southern Hemisphere Westerlies. It has been long known that the uneven supply of terrigenous sediment to the Chilean continental margin is related to the strong increase in onshore precipitation from north to south [10] (Fig. 1). Studies off northern and central Chile revealed that also qualitative variations of the terrigenous input can be used to trace latitudinal displacements of the Southern Westerlies and thus variations of the principal Southern Hemisphere atmospheric circulation pattern during the Late Quaternary [11–13].

In this paper we discuss the iron content and clay mineral record of a ^{14}C-accelerator mass spectrometry (AMS) dated high accumulation marine sediment core from the continental slope of southern Chile. Our geologic proxy data record pronounced climate variability on multi-centennial to millennial time-scales during the last ca. 7700 cal yr. We provide evidence, that rainfall variability of the Southern Hemisphere mid-latitudes is closely connected to changes within the tropical climate system while the relation to climate conditions in coastal Antarctica shifts during the late Holocene coinciding with the onset of the modern state of ENSO.

2. Investigation area

Marine sediment core GeoB 3313-1 was taken from a small forearc-basin on the upper continental slope at ca. 41°S off southern Chile (Fig. 1). The area is characterized by a 30–60 km wide shelf, which becomes significantly wider south of 42°S in the Chilean fjord region [10]. The upper continental slope is moderately inclined. Thick sheet-flow turbidites bury the Peru–Chile trench as a bathymetric feature in this region, while turbidity currents are more channelized on the upper slope [14].

The large-scale oceanic surface circulation off southern Chile is controlled by the Antarctic Circumpolar Current (Subantarctic Water) approaching the Chilean coast between 40 and 45°S, where it splits into the poleward Cape Horn Current and the equatorward Peru–Chile Current (Fig. 1) [15]. A poleward undercurrent (Gunther undercurrent) can be detected near the shelf edge at a water depth of 100–300 m. The Gunther undercurrent transports Equatorial Subsurface water to the south up to ca. 48°S (e.g. [16]) but diminishes in strength south of 33°S. Deeper currents include equatorward flowing Antarctic Intermediate Water (ca. 400–1200 m water depth) underlain by southward flowing Pacific Deep Water.

Three main physiographic features, the Coastal Ranges, the Chilean Longitudinal Valley, and the Andes characterize the continental hinterland around 41°S (Fig. 1). The Coastal Ranges with elevations of generally below 500 m are dominated by primarily low-grade metamorphic rocks [17]. The Central Valley is filled with up to 4000 m thick alluvial sediments. The Andes reach elevations of 2000–3000 m. The lower parts mainly consist of iron-poor plutonic basement rocks, while the high Andes are dominated by iron-rich basaltic to andesitic volcanics resulting from Pliocene to recent volcanic activity [14,17]. Various small rivers drain the Coastal Range within the study area. Larger rivers originating in the Andes flow into the ocean north (e.g. Rio Bueno; ca. 40°S) and south of the core position in the region of Puerto Montt. Therefore, terrigenous sediments on the continental slope can be expected to contain both a Coastal Range and Andean source rock signal.

The present climate of southern Chile around 41°S is characterized by humid temperate conditions with year round precipitation peaking in austral winter [18]. The area lies within the transition zone of the summer dry Mediterranean climate north of 37°S and year round humid con-

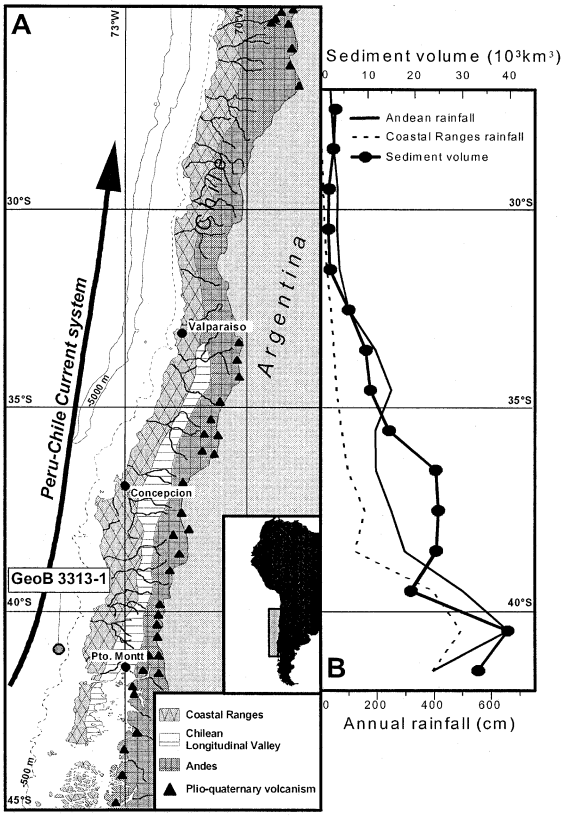

Fig. 1. (A) Map of Chile and the adjacent southeastern Pacific showing principal physiographic units. (B) Latitudinal distribution of rainfall in Chile (Andes and Coastal Range) and estimate of total volume of Cenozoic deposits on the Chilean continental margin based on data from Scholl et al. [10].

ditions with heavy precipitation south of 42°S. Rainfall originates from frontal passages of the Southern Westerlies and increases strongly to the south (Fig. 1) making the regional precipitation very sensitive to latitudinal shifts of this wind belt. Due to the orographic rising of moist Pacific air-masses, rainfall in the Andes is significantly higher than in low elevation areas. The track and intensity of cyclonic storms of the Southern Westerlies is controlled by the strength and latitudinal position of the subtropical anticyclone in the Southeast Pacific and the circum-Antarctic low pressure belt (e.g. [19]). Interannual rainfall variability, especially in central Chile, is strongly related to ENSO [20–22].

3. Material, methods and chronology

The data presented here have been obtained from gravity core GeoB 3313-1 (41°00′S; 74°27′W; water depth 852 m; core length 807 cm) which was recovered from the Chilean upper continental slope during the German R/V *Sonne* cruise 102 [23] (Fig. 1). Sediments consist of olive to dark olive clayey silts. The contents of biogenic sediment components are very low ($CaCO_3$: 3–12 wt%; opal: 2.1–4.5 wt%; C_{org}: 1.4–2.5 wt%).

3.1. Grain size analysis

The relative proportions of the sand (>63 μm), silt (2–63 μm), and clay fraction (<2 μm) have been determined on the carbonate and organic-matter-free sediment with a sample spacing of 10 cm. The sand fraction was separated by wet sieving and the remaining silt and clay fractions were split by an 8–12 times repeated settling procedure based on Stokes'law settling using Atterberg tubes.

3.2. Clay mineralogy

Clay mineral analysis was performed by X-ray diffraction on the carbonate-free Mg-saturated clay-fraction (<2 μm) following standard procedures described in detail by Petschick et al. [24]. Samples were taken with a spacing of 10 cm. Relative percentages of the four main clay mineral groups (smectite, illite, chlorite and kaolinite) were estimated by weighting integrated peak areas of characteristic basal reflections in the glycolated state with the empirical factors of Biscaye [25]. Smectite crystallinity was measured as the integral breadth (IB) of the glycolated 17Å smectite peak, which represents the breadth ($\Delta°2\theta$) of a rectangle of the same area and height as the peak. Repeated measurements of independently prepared mounts of the same sample indicate relative errors of clay mineral contents of $\pm 6.5\%$ and crystallinity parameters of $\pm 5.2\%$.

3.3. Iron contents

Iron contents were measured with a profiling

X-ray fluorescence scanner developed at the Netherlands Institute for Sea Research [26] in 1 cm intervals. In order to exclude dilution effects by biogenic particles, iron content data were converted into values corresponding to 100% terrigenous fraction.

3.4. Spectral analyses

Time-series analyses were carried out with the SPECTRUM software package [27]. Spectral analyses with this program are based on the Lomb–Scargle Fourier transformation method. As the Lomb–Scargle method does not require equidistant time-series, time-interpolation of the geological data was not applied. In order to distinguish the analyzed time-series from white noise, we calculated harmonic spectra and applied the Siegel test for testing the statistical significance.

3.5. Chronology

The age model of core 3313-1 is based on seven ^{14}C-AMS dates and linear interpolation between the dates. ^{14}C-AMS dates were determined on 10 mg carbonate (mixed planktonic foraminifera) at the Leibniz Laboratory (University of Kiel, Germany [28]). All ages are corrected for ^{13}C. As the core position lies significantly south of the Chilean upwelling zone [15] and north of the southern polar front, the ages are corrected for a reservoir age of 400 yr as the mean value for the Pacific Ocean at 40°S latitude [29]. The ^{14}C ages (Table 1) were converted to calendar years with the Calib 4.0 software [30]. The age–depth relation is shown in Fig. 2. Sedimentation rates are in the range of 100 cm/kyr on average. This age model results in an average time-resolution of ca. 10 yr for the iron content record (1 cm sampling interval) and ca. 100 yr for clay mineral records (10 cm sampling interval).

4. Paleoclimatic proxies

We use the iron content of the bulk sediment in combination with clay mineral data as indicators for qualitative changes in the terrigenous sediment input to the southern Chilean continental slope during the Holocene. Sediments in core GeoB 3313-1 consist of clayey silt. The relative proportions of sand, silt and clay do not vary significantly throughout the core (Fig. 3). Careful visual analyses of the sediments did not reveal any indications of turbiditic layers. Therefore, we assume that the primarily terrigenous sediments ($CaCO_3$: 3–12 wt%; opal: 2.1–4.5 wt%; C_{org}: 1.4–2.5 wt%) were deposited by hemipelagic processes without any significant contribution of turbidity currents or alteration by bottom currents.

As contents of biogenic components are very low and the data were converted into values corresponding to 100% terrigenous fraction, variations in iron contents are most likely induced by changes in the composition of the fluvial terrigenous sediment influx mainly due to variations in the relative contributions of source areas within the Coastal Ranges and the Andes (Fig. 1). The eolian input of iron to the core position can be excluded, as the area lies within the humid south-

Table 1
^{14}C-AMS dates of core GeoB 3313-1

Laboratory number	Core depth (cm)	^{14}C-AMS age (yr B.P)	± Error (yr)	Calibrated age (cal yr B.P.)
GeoB 3313-1:				
KIA 6794	33–43	195	30	260
KIA 6793	153–158	1220	30	1180
KIA 7231	258–268	1970	50	1980
KIA 5098	403–408	3460	40	3820
KIA 5097	503–513	4390	40	5040
KIA 7230	633–638	4830	60	5590
KIA 7229	753–758	6170	80	7090

KIA = Kiel.

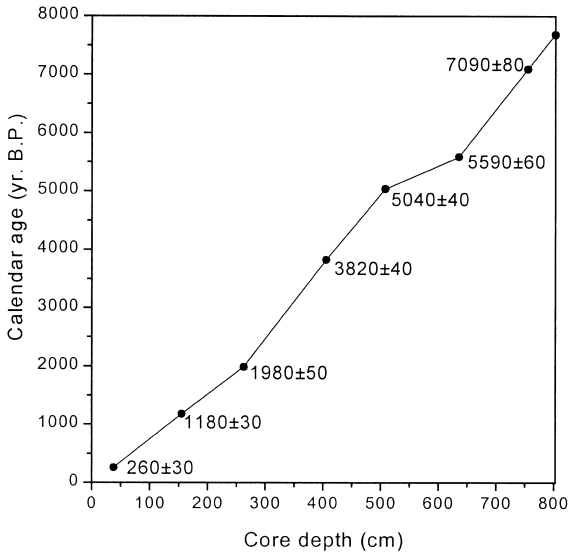

Fig. 2. Age–depth relation for core GeoB 3313-1 based on seven linearly interpolated ^{14}C-AMS dates. ^{14}C ages are shown in calendar years with a 400 yr reservoir effect correction. Measurements were performed at the Leibniz Laboratory AMS facility (University of Kiel, Germany).

ern westerly wind belt with nearly year-round onshore blowing winds.

The Coastal Ranges and the lower part of the Andes within the study area are dominated by comparatively iron-poor basement rocks, while the high Andes mainly consist of iron-rich volcanics. Our interpretations are based on the assumption that the relative influx of material from these two source regions is mainly determined by the amount of rainfall which is supported by analyses of marine surface sediments and stream samples [31] as well as Late Quaternary sediments from the northern and central Chilean slope [12,13].

Strong modern precipitation gradients and small-scale catchments of rivers in the Coastal Ranges and the lower parts of the Andes [18] (Fig. 1) make this area particularly sensitive to Holocene rainfall changes related to shifts of the Southern Westerlies. Modern rainfall changes of ca. 20% at Valdivia, a coastal station at 40°S, has been related to shifts of the mean position of the westerlies of only 1° of latitude [32]. The Andes on the other hand, even in central Chile receive comparatively high amounts of precipitation [18] (Fig. 1) making the sediment input from volcanic Andean sources less sensitive to rainfall changes and shifts of the westerlies. Therefore, we conclude that sediment input from volcanic Andean sources remained more or less constant throughout the Holocene. Thus, mainly the influx of material originating in the lower altitude regions with its smaller catchment areas has varied leading to a higher input of iron-poor material during more humid phases.

Our interpretation of the iron data is further supported by clay mineralogical data. Smectite, the principle clay mineral in marine sediments off southern Chile [33], predominates in sediments of core GeoB 3313-1 and comprises approximately 60–70% of the clay minerals (Fig. 4). Chlorite, illite, as well as kaolinite contents are

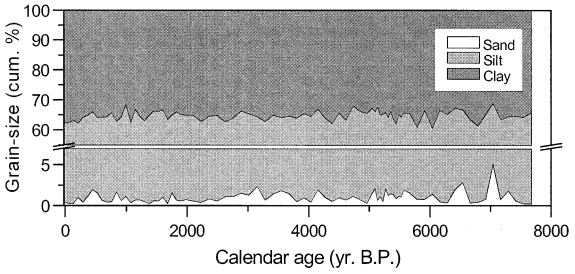

Fig. 3. Relative proportions of sand (>63 μm), silt (2–63 μm) and clay (<2 μm) in carbonate and organic-matter-free sediments of core GeoB 3313-1 (*y*-axis break from 7 to 55%). Low variability within the fine-grained sediments points to primarily hemipelagic sedimentation.

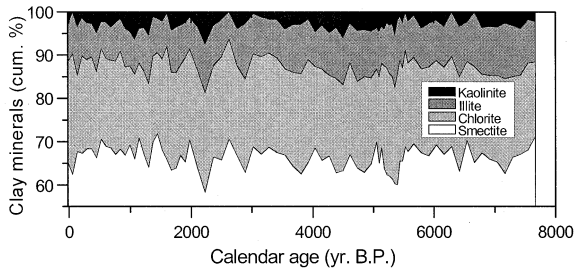

Fig. 4. Clay minerals in core GeoB 3313-1. Relative proportions of the four clay mineral groups smectite, chlorite, illite and kaolinite. Clay mineral assemblages are strongly dominated by smectite (ca. 60 to 70%).

low, in the range of 17–27, 6–13 and 0–8%, respectively (Fig. 4).

Though a detailed correlation of iron content and selected clay mineralogical data is not satisfactory (e.g. for reasons as differing time-resolution), the comparison of the smoothed data-sets reveals the following pattern (Fig. 5A–C): high iron contents parallel lower smectite contents and higher smectite crystallinities. Conversely, we find lower iron contents when smectite contents are higher and smectite crystallinities lower. Under temperate climate conditions, as in southern Chile, highly crystallized smectite forms on volcanic source rocks during the early stages of weathering, while low to medium crystallized smectite forms through more intensive chemical weathering processes in soils by degradation of primary minerals also on non-volcanic source rocks (pedogenic smectite) [34]. High iron contents coinciding with the occurrence of highly crystallized smectite can be best explained by a higher input of comparatively unweathered material from volcanic source areas in the high Andes. The iron content of terrigenous material mainly depends on the mineralogy and geochemistry of source rocks. Basaltic to andesitic source rocks generally contain high amounts of iron [35]. Additionally, highly crystallized smectite formed on basic volcanics is mostly dominated by nontronite [34], which is also characterized by high iron contents. On the other hand, we interpret lower iron contents paralleling increased amounts of low crystallized smectite, which is mostly iron-poor [34], as a higher contribution of material from the lower parts of the Andes and the Coastal Ranges during more humid time-spans. Compared to the high Andes, more acidic source rocks in those areas provide iron-poorer material to be transported to the ocean. These interpretations are consistent with source area shifts on longer time-scales during the last ca. 30 000 yr recorded off central Chile [12].

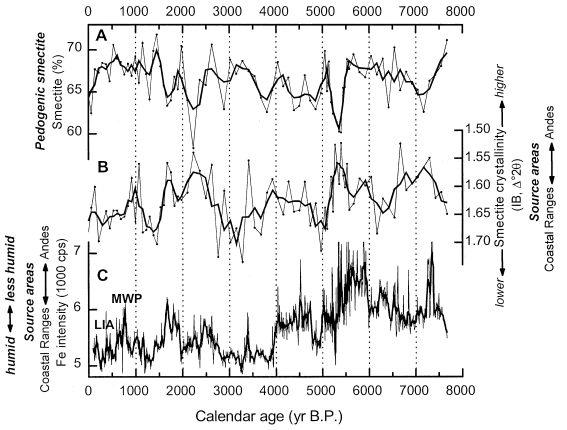

Fig. 5. Sedimentological paleoclimate proxy data of core GeoB 3313-1: (A) smectite content, (B) smectite crystallinity, and (C) iron content measured in counts per second (cps). Thin lines represent original data; thick lines are smoothed curves using a three-point and five-point moving average for clay mineral and iron content data, respectively. High smectite contents correlate to low smectite crystallinities ($r = 0.47$, $n = 151$). High smectite crystallinities correlate to high iron contents ($r = 0.55$, $n = 151$). All correlation coefficients are statistically significant on the 99.9% after applying a 50 yr time-resolution interpolation on the different records. Prominent late Holocene climate phases like the LIA and the MWP parallel humid/less humid periods in southern Chile.

5. Implications for Holocene climate change

In the following, we use the iron content record of core GeoB 3313-1 as a proxy for the history of regional rainfall in southern Chile during the last 7700 cal yr. As the modern rainfall distribution within the study area is clearly related to the latitudinal position of the Southern Westerlies [18], our record traces the Holocene location of one of the major Southern Hemisphere atmospheric circulation members.

The record is characterized by both a 'long-term' trend and significant shorter term variability on millennial to decadal time-scales (Fig. 5C). Generally less humid conditions (and thus more poleward located storm tracks of the westerlies) occurred from 7700 to 4000 cal yr B.P. (middle Holocene) peaking between 6000 and 5300 cal yr B.P. During the last 4000 cal yr (late Holocene), climate conditions were more humid on average but several century-scale peaks in iron content point to less humid intervals near 3400, 2500, from 1900 to 1600, and near 750 cal yr B.P. Spectral analyses indicate dominant rainfall variability at periods of 820, 950, 1340 and 1750 yr (Fig. 6B).

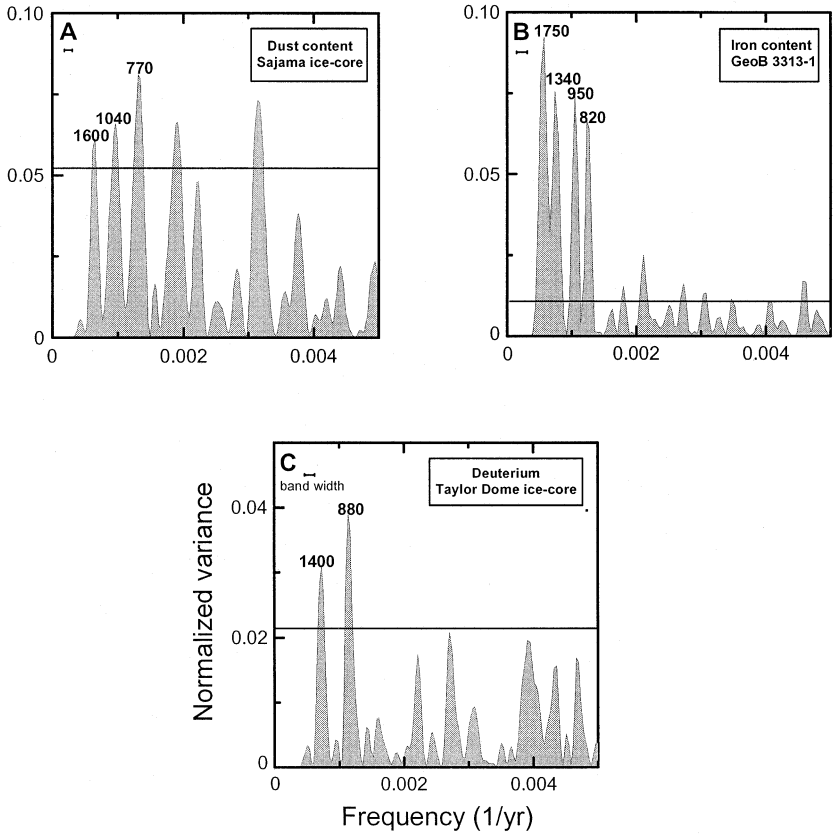

Fig. 6. Spectral analyses of paleoclimate records from tropical South America and coastal Antarctica performed with the SPECTRUM software [27]. Power spectra were calculated from harmonic analyses. Long-term trends within the data-sets have been removed by applying a 3000 yr high-pass filter. Horizontal lines indicate statistical significance of the Siegel test on the 95% level (except for B: 99% level). (A) Dust content record of the Sajama ice-core [41] (unsmoothed data 0–10 000 yr. B.P.; 6 dB bandwidth 0.00012 yr^{-1}; $\alpha = 0.05$). (B) Iron content data of core GeoB 3313-1 (unsmoothed data; 6 dB bandwidth 0.00016 yr^{-1}; $\alpha = 0.01$). (C) δD record of the Taylor Dome ice-core (unsmoothed data 0–8000 yr. B.P.; 6 dB bandwidth 0.000153 yr^{-1}; $\alpha = 0.05$). Labels indicate periods of spectral peaks in years.

5.1. Regional paleoclimate implications

The broad paleoclimatic pattern for southern Chile derived from our record is generally consistent with various terrestrial paleoclimate data-sets of mid-latitude Chile. Especially the Holocene 'long-term' trend which can be seen in our data (Fig. 5C), i.e. less humid conditions during the middle Holocene and more humid conditions in the late Holocene, can be found in both southern and central Chile. Glaciers in the southern Andes generally advanced during the late Holocene [36] and pollen data from Chiloé (42–43°S) indicate more humid conditions [37] compared to the middle Holocene. Similar results have been obtained from paleoenvironmental records of central Chile [12,38,39]. As central Chilean rainfall is also controlled by moisture originating from the Southern Westerlies, the data indicate that this wind-belt was generally located further south during the middle Holocene and further north in the late Holocene in mid-latitude Chile.

5.2. Forcing of shifts of the Southern Westerlies and wider implications

Modern climatological data suggest that the latitudinal position of the Southern Westerlies is

controlled by both high latitude conditions, i.e. around Antarctica, and changes in the tropics especially the strength and position of the subtropical anticyclone in the SE Pacific sector (e.g. [19]). For this reason, we tried to compare our proxy record of latitudinal shifts of the westerlies to paleoclimate data-sets of both Antarctica and tropical South America.

A general shift to more humid conditions after ca. 4000 cal yr. B.P. as recorded in mid-latitude Chile can also be found in many paleoclimate records of tropical South America especially on the Bolivian Altiplano (e.g. water level of Lake Titicaca [40] and Sajama ice-core data [41]) which is supposed to be related to stronger convective summer-rains due to increased summer insolation in the late Holocene (e.g. [40]). Changes in seasonal insolation might also have caused a general strengthening and equatorward shift of the Southern Westerlies during the late Holocene [42] consistent with our data.

The link between tropical and extratropical 'long-term' rainfall changes is most likely related to the tropical Hadley cell circulation over South America influencing both the strength and position of the SE Pacific anticyclone (and thus the position of the westerlies) as well as the strength of summer convection over the Bolivian Altiplano. Isolation-induced reduction of the intensity of the tropical Hadley cell during the late Holocene can therefore explain the similar 'long-term' rainfall changes in tropical and extratropical South America.

On multi-centennial to millennial-scales the water level record of Lake Titicaca [40] and most other paleoclimate records of the Altiplano region (e.g. [43,44]) do not show significant variations except for the Sajama ice-core dust content record [41]. We therefore compared the pronounced multi-centennial to millennial-scale variability in our record to the Sajama ice-core data. High dust contents in this ice-core are thought to record elevated snowlines and decreased ice accumulation pointing to more arid conditions on the Bolivian Altiplano probably induced by strengthened Hadley circulation and therefore less convective rainfall [41].

We first performed spectral analyses in order to define the dominant bands of variability in the Sajama dust content record and our Chilean data. The dominant periods in both records (1750, 1340, 950 and 820 yr versus 1600, 1040 and 770 yr; Fig. 6A,B) indicate a similar order of variability near 900 and 1500 yr. We therefore calculated two Gaussian band pass filters, one centered at 900 yr and a second centered at 1500 yr (Figs. 7 and 8). The 900 yr filters of the Sajama dust record and our Chilean data show a significant correlation implying that less humid conditions in southern Chile and more arid conditions on the Bolivian Altiplano correlate in that band (Fig. 7A,B). For the 1500 yr filter a significant correlation is present during the middle Holocene while in the late Holocene the amplitude of the 1500 yr cycle diminishes, especially in the Chilean record (Fig. 8A,B). These data suggest that also the reconstructed multi-centennial to millennial-scale changes in the latitudinal position of the Southern Westerlies during the Holocene are strongly related to the tropical climate system, i.e. the Hadley cell intensity.

Antarctic ice-core data reveal a non-uniform picture for the Holocene. While inland cores like Vostok generally show low variability during the Holocene with an early Holocene warm period ending at ca. 8000 yr B.P. [45], coastal sites like Taylor Dome show much larger isotopic changes with a warm period extending in the middle Holocene. The Late Holocene is characterized by generally cooler conditions [46]. The isotopic changes in the Taylor Dome ice-core are thought to not only reflect atmospheric temperature but also sea-ice cover around Antarctica [46]. The 'long-term' shift recorded in the Taylor Dome ice-core seems to be consistent with our data implying cooler conditions and increased sea-ice around Antarctica in the late Holocene when more humid conditions and equatorward located westerlies are recorded in Chile. In order to check whether this holds true also for the multi-centennial to millennial time-scale, we applied similar spectral analyses and band filter as described above to the deuterium isotope concentration (δD) record of the Taylor Dome ice-core [46]. Spectral analyses of the δD record reveal dominant periods near 880 and 1400 yr (Fig. 6C)

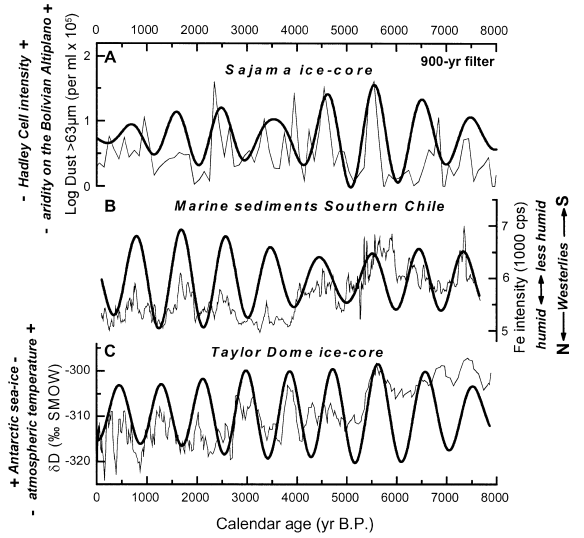

Fig. 7. Comparison with paleoclimate proxy records from tropical South America and coastal Antarctica (900 yr band). (A) Dust content of the Sajama ice-core (thin line) [41] interpreted as a proxy for the aridity of the Bolivian Altiplano and the Hadley cell intensity over the SE Pacific and tropical South America. (B) Iron content of marine sediments off southern Chile (this study) interpreted as a proxy for rainfall and the position of the Southern Westerlies (thin line = five-point moving average). (C) δD record of the Taylor Dome ice-core located (thin line = five-point moving average) interpreted as a proxy for atmospheric temperature in coastal Antarctica and the extension of Antarctic sea-ice [46]. Thick lines represent Gaussian band pass filter centered at 900 yr (0.00111 ± 0.0002 yr^{-1}). The band width chosen covers the dominant periodicities around 900 yr in the records as indicated by the spectral analyses (770, 820, 880, 950 and 1040 yr; Fig. 6). High iron contents in the Chilean record correlate to high dust contents in the Sajama ice-core in the 900 yr band ($r = 0.67$, $n = 151$). Correlation of iron contents to δD record of the Taylor Dome ice-core shifts from positive in the middle Holocene (high iron contents correlate to high δD values; $r = 0.38$, $n = 73$) to negative in the late Holocene (high iron contents correlate to low δD values; $r = -0.87$, $n = 78$). All correlation coefficients are statistically significant on the 99.9% level after applying a 50 yr time-resolution interpolation on the different records.

which again fall within the two band filters centered at 900 and 1500 yr. However, a positive correlation of the two band filters of the δD record and our Chilean record (i.e. similar to the 'long-term' trend) can only be found during the middle Holocene (Figs. 7B,C and 8B,C). Afterwards the records especially for the 900 yr band filters become antiphased (Fig. 7B,C).

Modern climatological analyses and long-term modelling for time-slices since the last glacial maximum (LGM) show a complex pattern of latitudinal shifts of the westerlies within different meridional sectors in response to high-latitude temperature gradients and sea-ice cover [47,48]. For the South American sector an equatorward displacement and a general latitudinal widening can be observed in the models for the LGM related to reduced temperatures and increased sea-ice around Antarctica consistent with our middle Holocene correlation. However, the obvious antiphase relationship of multi-centennial to millennial-scale variability between the Taylor Dome data and our Chilean record in the late Holocene points to different climate mechanisms being active during this time interval.

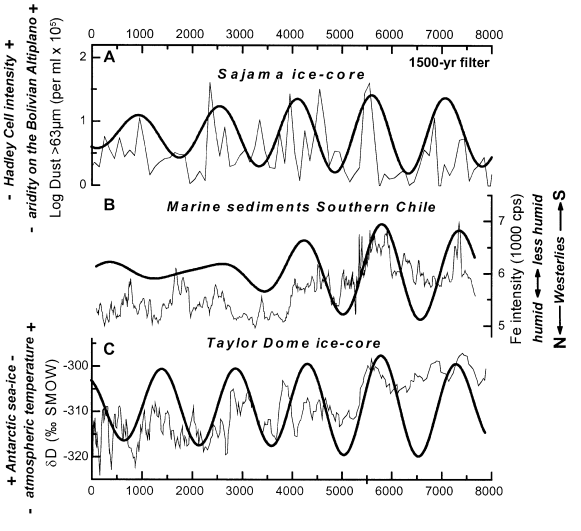

Fig. 8. Comparison with paleoclimate proxy records from tropical South America and coastal Antarctica (1500 yr band). Thin lines see Fig. 7. Thick lines represent Gaussian band pass filter centered at 1500 yr (0.000667 ± 0.0001 yr^{-1}). The band width chosen covers the dominant periodicities around 1500 yr in the records as indicated by the spectral analyses (1340, 1400, 1600 and 1750 yr; Fig. 6). Generally positive correlations of high iron contents in the Chilean record to both high dust content in the Sajama ice-core ($r = 0.61$, $n = 73$) and high δD values in the Taylor Dome ice-core ($r = 0.98$, $n = 73$) in the 1500 yr band during the middle Holocene. Variability of the Chilean record in the 1500 yr band diminishes significantly in the late Holocene. All correlation coefficients are statistically significant on the 99.9% level after applying a 50 yr time-resolution interpolation on the different records.

Such different mechanisms might be related not only to the different insolation characteristics, i.e. increased seasonality during the late Holocene compared to the early and middle Holocene [42] but also to the increased influence of ENSO in the late Holocene as seen in both 'long-term' paleo-ENSO-records (e.g. [49,50]) and long-term modelling studies [51]. Modern data show a strong influence of ENSO on both the behavior of Antarctic sea-ice [52] and on the latitudinal position of the westerlies in South America [20–22]. During the warm phase of ENSO (El Niño years), a weakening of the Southeast Pacific anticyclone results in a northward shift of the Southern Westerlies leading to wet anomalies in central Chile. Conversely, a strengthening and southward expansion of the anticyclone results in more poleward located westerly storm tracks reducing winter-rain in the Mediterranean climate zone of Chile during the La Niña state. One could speculate that the increasing amplitude of the 900 yr band filter at the expense of the 1500 yr band filter in our data during the late Holocene (Figs. 7B and 8B) might be related to a 'long-term' ENSO cycle which becomes more dominant. Proxy-data of environmental changes in southern California suggest 'long-term' ENSO-type oscillations with periods of ca. 1000 yr [53] quite near to the dominant 820 and 950 yr periodicities in our data.

5.3. Global paleoclimate implications

Within recent years increasing indications of a millennial-scale variability of Holocene climates emerged especially from paleoclimate records of the North Atlantic realm (e.g. [6]). These studies suggest a dominant periodicity of near-1500-yr for the major Holocene climate changes. Similar periods have also been found in changes within the monsoonal system (e.g. [7]). Interestingly, near-1500-yr cycles have not been found in the Greenland ice-core records which are dominated by cycles of 830–1050 yr [4,54] also present in changes of the North Atlantic circulation [55].

The cause of near-1500-yr cycles has been linked to an internal oscillation of the atmosphere–ocean system involving the deep water circulation in the North Atlantic (e.g. [6]) and possibly also the formation of Southern Ocean deep waters [56]. Cycles with a period of near 900 yr within the Greenland Gisp2 record have also been interpreted as an internal oscillation of the ocean–atmosphere system which is possibly triggered by salinity anomalies in the North Atlantic [4].

The influence of such changes in the global thermohaline circulation on the atmospheric circulation of the Southern Hemisphere mid-latitudes is difficult to assess and a direct correlation of the Northern Hemisphere records which are based on very different paleoclimate proxy records with varying time-resolutions to our Chilean data does not reveal statistically significant results. However, similar bands of variability around 1500 and 900 yr present in the high resolution Holocene records point to interhemispheric teleconnections. Our data show a close relation of the latitudinal shifts of the Southern Westerlies on these time-scales to changes in the tropical climate system possibly also including ENSO. Climate changes in the tropics, especially related to the hydrological balance, have often been suggested to be responsible for the interhemispheric transfer of paleoclimate signals during the last glacial and deglaciation (e.g. [57–59]). On the other hand, our comparison to the Taylor Dome ice-core record of Antarctica reveals a less consistent picture with an apparent shift from inphase to antiphase correlations especially of the 900 yr band variability in the late Holocene (Fig. 7B,C). This fits within the often contradictory results on the inphase or antiphase pattern of Antarctic climate changes versus Northern Hemisphere millennial-scale variations during the last glacial (e.g. [60,61] and also the late Holocene [56,62].

The probably most prominent climate event of the late Holocene is the Little Ice Age (LIA), a period of cold climate conditions from $\sim$1350 to 1880 A.D. especially around the North Atlantic [63] following the Medieval Warm Period (MWP). Our data show increased rainfall and an equatorward shift of the Southern Westerlies paralleling the LIA following decreased rainfall and a poleward shift coinciding with the MWP (Fig. 5C). Such a climate pattern is consistent with advancing glaciers in the Southern Andes and New Zea-

land during the LIA [63] and prolonged drought conditions in Patagonia during the MWP [64]. An explanation might be a synchronous enhancement of atmospheric circulation on both hemispheres during the LIA [65], which possibly also caused a mean equatorward shift of the westerlies [64]. Our data provide further indications that both the LIA and MWP were global climate events though the simple paradigm of global temperature anomalies during these events has been much questioned [66].

6. Conclusions

High sedimentation rates in marine sediments on the continental slope off southern Chile and a high sensitivity of regional precipitation to past climate change provide the opportunity to study Holocene rainfall variability on millennial to decadal time-scale induced by latitudinal shifts of the Southern Westerlies. Rainfall variability is recorded by changes in the composition of predominantly terrigenous sediments on the continental slope caused by varying relative source rock contributions of the Chilean Coastal Range and the Andes.

Superimposed on a 'long-term' precipitation pattern, i.e. generally less humid conditions occurred during the middle Holocene (7700 to 4000 cal yr B.P.) compared to the late Holocene (4000 cal yr B.P. to present), variability on different shorter time-scales is recorded. Especially the 'long-term' pattern is generally consistent with other regional paleoclimate data-sets from southern South America.

On a continental scale, Holocene shifts of the Southern Westerlies on multi-centennial to millennial time-scales (900 and 1500 yr bands) appear to be closely related to changes within the tropical climate system (i.e. Hadley cell intensity). A comparison of the Chilean data to ice-core data from coastal Antarctica revealed a change of the correlation from poleward shifts of the westerlies in phase with warmer temperatures/decreased sea-ice during the middle Holocene to an antiphase relationship in the late Holocene. This shift might be related to the onset of the modern state of ENSO at the beginning of the late Holocene.

Similar bands of variability as in the Chilean data can be found in many high resolution climate records from the Northern Hemisphere which points to interhemispheric connections of climate change on multi-centennial to millennial time-scales. The close connection of shifts of the Southern Westerlies to changes in the tropical climate system suggests a major role of the tropics for the interhemispheric transfer of climate signals on these time-scales.

To what extent external factors (variations in solar activity have been related to the origin of the near-1500-yr cycle [67] and orbital parameters display a periodicity in the range of 900 yr [68]) and/or internal ocean–atmosphere variability (global thermohaline circulation, ENSO) are the ultimate forcing mechanisms of global Holocene climate changes can presently not be decided. Further studies on high resolution Holocene sequences especially from the Southern Hemisphere are still necessary for a better understanding of the interhemispheric pattern of Holocene climate change and the role of 'long-term' changes of the ENSO-system.

Acknowledgements

We thank the captain and crew of RV *Sonne* for their excellent help in collecting the samples. B. Diekmann, G. Kuhn, R. Fröhlking, S. Janisch and H. Rhodes at the Alfred Wegener Institute in Bremerhaven are acknowledged for analytical assistance. Financial support was provided by the German Bundesministerium für Bildung und Forschung through funding the project *CHIPAL* (03G0102A).***[FA]***

References

[1] W. Dansgaard, S.J. Johnsen, H.B. Clausen, D. Dahl-Jensen, N.S. Gundestrup, C.U. Hammer, C.S. Hvidberg, J.P. Steffensen, A.E. Sveinbjörnsdottir, J. Jouzel, G. Bond, Evidence for general instability of past climate from a 250-kyr ice-core record, Nature 364 (1993) 218–220.

[2] G.H. Denton, W. Karlen, Holocene climatic variations; their pattern and possible cause, Quat. Res. 3 (1973) 155–205.
[3] S.R. O'Brien, P.A. Mayewski, L.D. Meeker, D.A. Meese, M.S. Twickler, S.I. Whitlow, Complexity of Holocene climate as reconstructed from a Greenland ice core, Science 270 (1995) 1962–1964.
[4] M. Schulz, A. Paul, Holocene climate variability on centennial-to-millennial time-scales: 1. Climate records from the North Atlantic realm, in: W. Berger, G. Wefer (Eds.), Past Climate and its Significance for Human History in NW Europe, the Last 10 000 Years, Springer, 2000, in press.
[5] J.C. Stager, P.A. Mayewski, Abrupt Early to Mid-Holocene climatic transition registered at the equator and the poles, Science 276 (1997) 1834–1836.
[6] G.C. Bond, W. Showers, M. Elliot, M. Evans, R. Lotti, I. Hajdas, G. Bonani, S. Johnson, The North Atlantic's 1–2 kyr climate rhythm: relation to Heinrich events, Dansgaard/Oeschger Cycles and the Little Ice Age, in: P.U. Clark, R.S. Webb, L.D. Keigwin (Eds.), Mechanisms of Global Climate Change at Millennial Time-scales, American Geophysical Union, Washington, DC, 1999, pp. 35–58.
[7] A. Sarkar, R. Ramesh, B.L.K. Somayajulu, R. Agnihotri, A.J.T. Jull, G.S. Burr, High resolution Holocene monsoon record from the eastern Arabian Sea, Earth Planet. Sci. Lett. 177 (2000) 209–218.
[8] P.U. Clark, R.S. Webb, L.D. Keigwin, Mechanisms of Global Climate Change at Millennial Time-scales, American Geophysical Union, Washington, DC, 1999.
[9] A.C. Clement, M. Cane, A role for the tropical Pacific coupled ocean–atmosphere system on Milankovitch and millennial timescales. Part I: Modelling study of tropical Pacific variability, in: P.U. Clark, R.S. Webb, L.D. Keigwin (Eds.), Mechanisms of Global Climate Change at Millennial Time-scales, American Geophysical Union, Washington, DC, 1999, pp. 363–371.
[10] D.W. Scholl, M.N. Christensen, R. Von Huene, M. Marlow, Peru–Chile Trench. Sediments and sea-floor spreading, Geol. Soc. Am. Bull. 81 (1970) 1339–1360.
[11] F. Lamy, D. Hebbeln, G. Wefer, Late Quaternary precessional cycles of terrigenous sediment input off the Norte Chico, Chile (27.5°S) and paleoclimatic implications, Palaeogeograph. Palaeoclimatol. Palaeoecol. 141 (3–4) (1998) 233–251.
[12] F. Lamy, D. Hebbeln, G. Wefer, High resolution marine record of climatic change in mid-latitude Chile during the last 28 000 years based on terrigenous sediment parameters, Quat. Res. 51 (1999) 83–93.
[13] F. Lamy, J. Klump, D. Hebbeln, G. Wefer, Late Quaternary rapid climate change in northern Chile, Terra Nova 12 (2000) 8–13.
[14] T. Thornburg, L.D. Kulm, Sedimentation in the Chile Trench: Petrofacies and provenance, J. Sediment. Petrol. 57 (1987) 55–74.
[15] P.T. Strub, J.M. Mesias, V. Montecino, J. Ruttlant, S. Salinas, Coastal ocean circulation off Western South America, in: A.R. Robinson, K.H. Brink (Eds.), The Global Coastal Ocean. Regional Studies and Syntheses, Wiley, New York, 1998, pp. 273–315.
[16] T.R. Fonseca, An overview of the Poleward Undercurrent and upwelling along the Chilean coast, in: S.J. Neshyba, C.N.K. Mooers, R.L. Smith, R.T. Barber (Eds.), Poleward Flows along Eastern Ocean Boundaries, Springer, New York, 1989.
[17] W. Zeil, Südamerika, Enke, Stuttgart, 1986.
[18] A. Miller, The climate of Chile, in: W. Schwerdtfeger (Ed.), World Survey of Climatology, vol. 12, Elsevier, Amsterdam, 1976, pp. 113–145.
[19] V. Markgraf, Past climates of South America, in: J.E. Hobbs, J.A. Lindesay, H.A. Bridgman (Eds.), Climates of the Southern Continents: Present, Past and Future, Wiley, New York, 1998, pp. 107–134.
[20] R.S. Cerveny, Present climates of South America, in: J.E. Hobbs, J.A. Lindesay, H.A. Bridgman (Eds.), Climates of the Southern Continents: Present, Past and Future, Wiley, New York, 1998, pp. 107–134.
[21] J. Ruttland, H. Fuenzalida, Synoptic aspects of the central Chile rainfall variability associated with the Southern Oscillation, Int. J. Climatol. 11 (1991) 63–76.
[22] D.J. Karoly, Southern Hemisphere circulation features associated with El Niño-Southern Oscillation events, J. Climatol. 2 (1989) 1239–1252.
[23] D. Hebbeln, G. Wefer and cruise participants, Cruise Report of R/V *Sonne* Cruise 102, Valparaiso–Valparaiso, 9.5.95–28.6.95, Universität Bremen, Bremen, 1995.
[24] R. Petschick, G. Kuhn, F. Gingele, Clay mineral distribution in surface sediments of the South Atlantic: sources, transport and relation to oceanography, Mar. Geol. 130 (1996) 203–229.
[25] P.E. Biscaye, Mineralogy and sedimentation of recent deep-sea clay in the Atlantic Ocean and adjacent seas and oceans, Geol. Soc. Am. Bull. 76 (1965) 803–832.
[26] J.H.F. Jansen, S.J. Van der Gaast, B. Koster, A. Vaars, CORTEX, a shipboard XRF-scanner for element analyses in split sediment cores, Mar. Geol. 151 (1998) 143–153.
[27] M. Schulz, K. Stattegger, SPECTRUM: spectral analysis of unevenly spaced paleoclimatic time series, Comput. Geosci. 23 (1997) 929–945.
[28] M.J. Nadeau, M. Schleicher, P.M. Grootes, H. Erlenkeuser, A. Gottolong, D.J.W. Mous, J.M. Sarnthein, N. Willkomm, The Leibniz-Labor AMS facility at the Christian-Albrechts University, Kiel, Germany, Nucl. Instrum. Methods Phys. Res. 123 (1997) 22–30.
[29] E. Bard, Correction of accelerator mass spectrometry ^{14}C ages measured in planktonic foraminifera: paleoceanographic implications, Paleoceanography 3 (1988) 635–645.
[30] M. Stuiver, P.J. Reimer, Extended ^{14}C data-base and revised Calib 3.0 ^{14}C age calibration program, Radiocarbon 35 (1993) 215–230.
[31] J. Klump, D. Hebbeln, G. Wefer, The impact of sediment provenance on barium-based productivity estimates, Mar. Geol. 169 (2000) 259–271.

[32] A.B. Pittock, Rainfall and the general circulation, in: Preprints Int. Conf. Eather Modification, Am. Meteor. Soc., Canberra, 1971, pp. 330–338.
[33] F. Lamy, D. Hebbeln, G. Wefer, Terrigenous sediment supply along the Chilean continental slope modern regional patterns of texture and composition, Geol. Rundsch. 87 (1998) 477–494.
[34] H. Chamley, Clay Sedimentology, Springer, Berlin, 1989.
[35] R.W. LeMaitre, The chemical variability of some common igneous rocks, J. Petrol. 17 (1976) 589–637.
[36] F. Röthlisberger, 10000 Jahre Gletschergeschichte der Erde, Sauerländer, Aarau, 1986.
[37] C. Villagrán, Glacial climates and their effects on the history of the vegetation of Chile: a synthesis based on palynological evidence from Isla de Chiloé, Rev. Palaeobot. Palynol. 65 (1990) 17–24.
[38] C.J. Heusser, Ice age vegetation and climate of subtropical Chile, Palaeogeograph. Palaeoclimatol. Palaeoecol. 80 (1990) 107–127.
[39] C. Villagrán, J. Varela, Palynological evidence for increased aridity on the Central Chilean coast during the Holocene, Quat. Res. 34 (1990) 198–207.
[40] S.L. Cross, P.A. Baker, G.O. Seltzer, S.C. Fritz, R.B. Dunbar, A new estimate of the Holocene lowstand level of Lake Titicaca, central Andes, and implications for tropical pelaeohydrology, Holocene 10 (2000) 21–32.
[41] L.G. Thompson, M.E. Davis, E. Mosley-Thompson, A. Sowers, K.A. Henderson, V.S. Zagorodov, P.-N. Lin, V.N. Mikhalenko, R.K. Campen, J.F. Bolzan, J. Cole-Dai, B. Francou, A 25 000 year tropical climate history from the Bolivian ice cores, Science 282 (1998) 1858–1864.
[42] V. Markgraf, J.R. Dodson, P.A. Kershaw, M.S. McGlone, N. Nicholls, Evolution of late Pleistocene and Holocene climates in the circum-South Pacific land areas, Climate Dyn. 6 (1992) 193–211.
[43] B.L. Valero-Garcés, M. Grosjean, A. Schwalb, M. Geyh, B. Messerli, K. Kelts, Limnogeology of Laguna Miscanti evidence for mid to late Holocene moisture changes in the Atacama Altiplano (Northern Chile), J. Paleolimnol. 16 (1996) 1–21.
[44] M. Grosjean, Paleohydrology of the Laguna Lejia (north Chilean Altiplano) and climatic implications for late-glacial times, Palaeogeograph. Palaeoclimatol. Palaeoecol. 109 (1994) 89–100.
[45] P. Ciais, J.R. Petit, J. Jouzel, C. Lorius, N.I. Barkov, V. Lipenkov, V. Nicolaiev, Evidence for an early Holocene climatic optimum in the Antarctic deep ice-core record, Climate Dyn. 6 (1992) 169–177.
[46] E.J. Steig, C.H. Hart, J.W.C. White, W.L. Cunningham, M.D. Davis, E.S. Satzman, Changes in climate, ocean and ice-sheet conditions in the Ross embayment, Antarctica, at 6 ka, Ann. Glaciol. 27 (1998) 305–310.
[47] P.J. Valdes, South American palaeoclimate model simulations how reliable are the models?, J. Quat. Sci. 15 (2000) 357–369.
[48] K.-H. Wyrwoll, B. Dong, P. Valdes, On the position of southern hemiphere westerlies at the Last Glacial Maximum: an outline of AGCM simulation results and evaluation of their implications, Quat. Sci. Rev. 19 (2000) 881–898.
[49] J. Shulmeister, B.G. Lees, Pollen evidence from tropical Australia for the onset of an ENSO-dominated climate at ca. 4000 B.P., Holocene 5 (1995) 10–18.
[50] M.S. McGlone, A.P. Kershaw, V. Markgraf, El Niño/Southern Oscillation climatic variability in Australasian and South American paleoenvironmental records, in: H.F. Diaz, V. Markgraf (Eds.), El Niño: Historical and Paleoclimatic aspects of the Southern Oscillation, Cambridge University Press, Cambridge, 1992, pp. 435–462.
[51] A.C. Clement, R. Seager, M.A. Cane, Orbital controls on the El Niño/Southern Oscillation and the tropical climate, Paleoceanography 14 (1999) 441–456.
[52] I. Simmonds, T.H. Jacka, Relationship between the interannual variability of Antarctic sea-ice and the Southern Oscillation index, J. Climate 8 (1995) 637–647.
[53] L.E. Heusser, F. Sirocko, Millenial pulsing of environmental change in southern California from the past 24 k.y. a record of Indo-Pacific ENSO events?, Geology 25 (1997) 243–246.
[54] P.M. Grootes, M. Stuiver, Oxygen 18/16 variability in Greenland snow and ice with 10^{-3} to 10^{5}-year time resolution, J. Geophys. Res. 102 (1997) 26455–26470.
[55] M.R. Chapman, N.J. Shackleton, Evidence of 550-year and 1000-year cyclicities in North Atlantic circulation pattern during the Holocene, Holocene 10 (2000) 287–291.
[56] W.S. Broecker, S. Sutherland, T.-H. Peng, A possible 20th-century slowdown of Southern Ocean deep water formation, Science 286 (1999) 1132–1135.
[57] G.H. Denton, C.J. Heusser, T.V. Lowell, P.J. Moreno, B.G. Andersen, L.E. Heusser, C. Schlüchter, D.R. Marchant, Interhemispheric linkage of paleoclimate during the last glaciation, Geograf. Ann. 81A (1999) 107–153.
[58] E. Bard, F. Rostek, C. Sonzogni, Interhemispheric sychrony of the last deglaciation inferred from alkenone palaeothermometry, Nature 385 (1997) 707–710.
[59] T.V. Lowell, C.J. Heusser, B.G. Andersen, P.I. Moreno, A. Hauser, L.E. Heusser, C. Schlüchter, D.R. Marchant, G.H. Denton, Interhemispheric correlation of Late Pleistocene glacial events, Science 269 (1995) 1541–1549.
[60] T. Blunier, J. Chappellaz, J. Schwander, A. Dällenbach, B. Stauffer, T.F. Stocker, D. Raynaud, J. Jouzel, H.B. Clausens, C.U. Hammer, S.J. Johnsen, Asynchrony of Antarctic and Greenland climate change during the last glacial period, Nature 394 (1998) 739–743.
[61] E.J. Steig, E.J. Brook, J.W.C. White, C.M. Sucher, M.L. Bender, S.J. Lehman, D. Morse, E.D. Waddington, G.D. Clow, Synchronous climate changes in Antarctica and the North Atlantic, Science 282 (1998) 92–95.
[62] E.W. Domack, P.A. Mayewski, Bi-polar ocean linkages evidence from late-Holocene Antarctic marine and Greenland ice-core records, Holocene 9 (1999) 247–251.
[63] J.M. Grove, The Little Ice Age, Methuen, London, 1988.
[64] S. Stine, Extreme and persistent drought in California and

Patagonia during mediaeval time, Nature 369 (1994) 546–549.

[65] K.J. Kreutz, P.A. Mayewski, L.D. Meeker, M.S. Twickler, S.I. Whitlow, I.I. Pittalwala, Bipolar changes in atmospheric circulation during the Little Ice Age, Science 277 (1997) 1294–1296.

[66] R.S. Bradley, Climate paradigms for the last millenium, PAGES Newslett. 8 (1) (2000) 2–3.

[67] B. van Geel, O.M. Raspopov, H. Renssen, J. van der Plicht, V.A. Dergachev, H.A.J. Meijer, The role of solar forcing upon climate change, Quat. Sci. Rev. 18 (1999) 331–338.

[68] M.R. Loutre, A. Berger, P. Bretagnon, P.-L. Blanc, Astronomical frequencies for climate research at the decadal to century time scale, Climate Dyn. 7 (1992) 181–194.